Antiviral Research 167 (2019) 13–24

Contents lists available at ScienceDirect

Antiviral Research

journal homepage: www.elsevier.com/locate/antiviral

Research paper

Antiviral activity of pinocembrin against Zika virus replication

Jia Le Lee[a], Marcus Wing Choy Loe[a], Regina Ching Hua Lee[a], Justin Jang Hann Chu[a,b,*]

[a] Laboratory of Molecular RNA Virology and Antiviral Strategies, Department of Microbiology, Yong Loo Lin School of Medicine, National University Health System, National University of Singapore, Singapore

[b] Institute of Molecular and Cell Biology, Agency for Science, Technology and Research (A*STAR), Singapore

ARTICLE INFO

Keywords:
Zika
Antiviral
Flavonoids
Natural compounds
Screening

ABSTRACT

Zika virus (ZIKV) is a mosquito-borne virus that has garnered a lot of attention in recent years, due to the explosive epidemic from 2014 to 2016. Since its introduction in the Americas in late 2014, ZIKV has spread at an unprecedented rate and scale throughout the world and infected millions of people. Its infection has also been associated with severe neurological disorders like Guillain-Barré syndrome and microcephaly in fetuses. Despite these, there is currently no approved antiviral against ZIKV. In this study, an immunofluorescence-based high throughput screen was conducted on a library of 483 flavonoid derivatives to identify potential anti-ZIKV compounds. Flavonoids, which are natural polyphenolic compounds found in plants, represent an attractive source of antivirals due to their abundance in food and expected low toxicity. From the primary screen, three hits were selected for validation by cell viability and viral plaque reduction assays. Pinocembrin, a flavanone found in honey, tea and red wine, was chosen for downstream studies as it exhibited the strongest inhibition of ZIKV infection in human placental JEG-3 cells (IC_{50} = 17.4 μM). Time-course studies revealed that pinocembrin acts on post-entry process(es) of the ZIKV replication cycle. Furthermore, pinocembrin inhibits viral RNA production and envelope protein synthesis based on quantitative reverse transcription-PCR (qRT-PCR) and Western blot analyses. This study has demonstrated for the first time the *in vitro* anti-ZIKV activity of pinocembrin.

1. Introduction

Zika virus (ZIKV) is an arthropod-borne virus belonging to the *Flavivirus* genus of the *Flaviviridae* family. The *Flaviviridae* family comprises of many well-known human and animal pathogens like dengue virus (DENV), yellow fever virus and West Nile virus (Gould and Solomon, 2008).

ZIKV was first isolated from a rhesus macaque in the Zika forest of Uganda in 1947 (Dick et al., 1952). Human ZIKV infections remained sporadic until 2007, when a massive outbreak was reported in Yap Island, Micronesia and nearly 75% of its population was infected (Duffy et al., 2009). Subsequently, another major ZIKV epidemic occurred from 2013 to 2014 in French Polynesia (Song et al., 2017). However, the event that cast the spotlight back onto ZIKV was the recent explosive epidemic from 2014 to 2016. First detected in late 2014 in Brazil, the virus spread at an unprecedented rate and scale throughout Central and South America and the Caribbean and was subsequently imported to many countries beyond the region, such as in the Pacific Islands and Southeast Asia. Due to the large scale of the epidemic and an observed increase in ZIKV-related microcephaly cases, the World Health Organization (WHO) declared ZIKV a global health emergency in February 2016 (WHO, 2016).

ZIKV infection is usually mild and self-limiting, characterized by fever, rash, arthralgia and conjunctivitis (Burke et al., 2016). While these symptoms are similar to that of other flaviviral infections, ZIKV infection has also been associated with severe disorders like Guillain-Barré syndrome and meningoencephalitis in infected adults and congenital defects in affected infants (WHO, 2016). Dramatic increases in microcephaly cases have been observed during the Brazil ZIKV epidemic and in French Polynesia retrospectively (Cauchemez et al., 2016; Kleber de Oliveira et al., 2016).

Despite these, no approved antiviral against ZIKV is available and treatment strategies are generally targeted at symptomatic relief using analgesics and antipyretics (Saiz and Martín-Acebes, 2017). To date, many countries in the world remain at risk of ZIKV outbreaks due to their high volumes of trade and travel and the prevalence of *Aedes* spp. vectors (CDC, 2018). Considering this and the positive correlation between ZIKV and severe disease outcomes, there therefore remains an urgent need to develop effective and potent antivirals against ZIKV to control future outbreaks.

* Corresponding authorLaboratory of Molecular RNA Virology and Antiviral Strategies, Department of Microbiology, Yong Loo Lin School of Medicine, National University Health System, National University of Singapore, Singapore.

E-mail address: miccjh@nus.edu.sg (J.J.H. Chu).

https://doi.org/10.1016/j.antiviral.2019.04.003
Received 7 October 2018; Received in revised form 25 March 2019; Accepted 1 April 2019
Available online 05 April 2019

An understanding of the ZIKV replication cycle is imperative in identifying potential targets for the development of antivirals. ZIKV is an enveloped virus with a single-stranded positive-sense RNA genome of about 10.7 kb long (Kuno and Chang, 2007). The open reading frame of its genome encodes a single polyprotein, which is post-translationally cleaved to yield the 3 structural proteins, the envelope (E), capsid (C) and pre-membrane (prM) proteins, and the 7 non-structural proteins, NS1, NS2A, NS2B, NS3, NS4A, NS4B, NS5 (Saiz et al., 2016). During infection, the ZIKV E protein facilitates binding of the virus to the host receptors and the virus enters the target cell via clathrin-mediated endocytosis. Acidification of endosome promotes membrane fusion and viral RNA release into the cytoplasm (Stiasny et al., 2011). The positive-sense RNA is translated into a single polyprotein by ribosomes at the surface of the host endoplasmic reticulum (ER). The single polyprotein is then post-translationally processed by viral NS2B/NS3 protease and host cell signalase, to yield the viral proteins (Lei et al., 2016). Genome replication occurs on virus-induced membranes derived from the ER and is mediated by the NS5 RNA-dependent RNA polymerase (Fernandez-Garcia et al., 2009). Viral structural proteins and the replicated genome then assemble into immature virions which bud into the ER and travel through the trans-Golgi network. Maturation of virions occurs through Furin-mediated cleavage of prM (Roby et al., 2015). Mature virions are then released via exocytosis, where they infect other susceptible cells.

In this study, an immunofluorescence-based high throughput screening (HTS) assay using human placental JEG-3 cells was developed to screen for potential inhibitors of ZIKV replication. While several research groups have conducted HTS on different compound libraries to identify ZIKV inhibitors, this is the first HTS assay that has been done on the flavonoid derivatives library. Flavonoids are a class of plant secondary metabolites found in many fruits and vegetables (Panche et al., 2016). They have gained medicinal interest over the years due to the wide range of pharmacological activities they exhibit, which include anti-oxidant, anti-inflammatory, antiviral, anti-bacterial and anti-carcinogenic effects (Cushnie and Lamb, 2011; Kaul et al., 1985; Rice-Evans, 2001; Sharma et al., 2011). Furthermore, they are widely available and have expected low toxicity. It is therefore important for us to assess the potential anti-ZIKV activities of flavonoids during the process of discovering an antiviral for the virus.

The primary screen was conducted on a library of 483 flavonoid derivatives with nine core structures that can be found at http://www.timtec.net/flavonoid-derivatives.html. Following validation of three of the top hits, pinocembrin was chosen for further studies due to its observed potency against ZIKV infection and novelty as an antiviral. Pinocembrin is a flavanone found in a wide array of plants including *Pinus* heartwood and *Eucalyptus*, and food products like honey, red wine and tea (Rasul et al., 2013). Various experiments were performed to understand the possible mechanism of action of the anti-ZIKV activity of pinocembrin.

2. Materials and methods

Cell Lines and Viruses *Aedes albopictus* C6/36 cells (ATCC CRL-1660™), baby hamster kidney cells (BHK-21; ATCC CCL-10™), human placenta choriocarcinoma JEG-3 cells (ATCC HTB-36™), human cervical carcinoma HeLa cells (ATCC CCL-2™), human hepatoma Huh7 cells (Dr Priscilla Yang, Harvard Medical School), human embryonic kidney HEK293T cells (ATCC CRL-11268™) and human muscle rhabdomyosarcoma cells (RD; ATCC CCL-136™) were used in this study. C6/36 cells were cultured in L-15 medium (Sigma-Aldrich) supplemented with 10% heat-inactivated fetal calf serum (HI-FCS; Capricorn Scientific) at 28 °C without carbon dioxide (CO_2) supplementation. BHK-21 cells were cultured in Roswell Park Memorial Institute 1640 medium (RPMI-1640; Sigma-Aldrich) supplemented with 10% FCS while JEG-3, HeLa, Huh7, HEK293T and RD cells were cultured in Dulbecco's Modified Eagle's medium (DMEM; Sigma-Aldrich) supplemented with 10% HI-FCS. Both media were buffered with 2 g of sodium hydrogen carbonate and all cells were incubated in a humidified incubator at 37 °C with 5% CO_2. Four different viruses were used in this study. They are ZIKV PRVABC59 Puerto Rico strain (GenBank accession no. KU501215.1), DENV2 New Guinea C strain (GenBank accession no. KM204118.1), Chikungunya virus (CHIKV) strain SGEHI-CHD122508 (GenBank accession no. FJ445502.2) and Enterovirus-A71 (EV-A71, GenBank accession no. AF316321.2). ZIKV, DENV2 and CHIKV were propagated in C6/36 cells while EV-A71 was propagated in RD cells. The viruses were harvested and stored in cryovials at −80 °C until required.

Flavonoid Derivatives Library The primary screen of antiviral effect against ZIKV infection was conducted on a library of 483 flavonoid derivatives (TimTec). The complete list of compounds can be found at http://www.timtec.net/flavonoid-derivatives.html. The compounds were first diluted with dimethyl sulfoxide (DMSO) in 96-well plates to a stock concentration of 20 mg/ml. The compounds were then further diluted with serum-free media in daughter plates to 200μg/ml. The daughter plates were stored at −20 °C until required.

Primary Screen The flavonoid derivatives library was screened on JEG-3 cells seeded in 96-well plates (Corning) at a density of 1.3×10^4 cells/well. The cells were infected with ZIKV at a multiplicity of infection (MOI) of 5 for 1 h at 37 °C, with gentle rocking every 15 min. After which, the cells were washed twice with phosphate buffered saline (1 X PBS) to remove the unbound viruses. Compounds of the library were then added to the cells at a final concentration of 20μg/ml. Cells treated with 0.1% DMSO and 80 μM ribavirin served as the vehicle control and positive control respectively. The treated plates were incubated overnight at 37 °C, 5% CO_2. After the incubation, the cells were fixed with ice-cold methanol (Sinopharm Chemical) before being washed thrice with 1 x PBS. The fixed cell monolayer was then rehydrated in 50 μL of 1 X PBS. Indirect immunofluorescence assay was then conducted. The fixed cell monolayers were first incubated with ZIKV anti-E-protein DIII ZV-67 1° antibody (Absolute Antibody) at 1:100 dilution for 1 h at 37 °C. After incubation and washing, the cells were incubated with anti-rabbit fluorescein isothiocyanate (FITC) 2° antibody (Merck Millipore) at 1:200 dilution for 1 h at 37 °C. Finally, the cells were incubated with DAPI (Sigma-Aldrich) at $1:1 \times 10^5$ dilution for 15 min at room temperature. Cells were washed twice with 1 X PBS and stored in 100 μL of 1 X PBS.

Data Acquisition Images of the stained cells were taken using the Operetta High-Content Imaging System with Harmony High-Content Imaging and Analysis Software (PerkinElmer). For each well, images of the central region were taken at 20× magnification for both the DAPI and fluorescein channels. The images were subsequently analyzed using the Cell Profiler software (Carpenter et al., 2006). The DAPI signal and fluorescein signal correspond to the number of live cells and extensiveness of ZIKV infection in each well respectively. The percentage infection was then determined by the formula: $\frac{Fluorescein\ signal\ count}{DAPI\ signal\ count} \times 100\%$. Subsequently, the percentage inhibition of viral replication was determined with the formula: $\frac{(IRv - IR_T)}{IRv} \times 100\%$, where IR_V refers to the infection rate of vehicle controls [ZIKV-infected, 0.1% DMSO-treated cells] while IR_T refers to the infection rate of ZIKV-infected, flavonoid-treated cells. Compounds that exhibited 50% or more inhibition of ZIKV infection were identified as positive hits from the primary screen. A number of these hits were then selected for further evaluation of their antiviral properties.

The robustness of the primary screening assay was determined using the Z-factor. The Z-factor is a statistical parameter that measures the ability of an assay to identify hits with high fidelity (Zhang et al., 1999). JEG-3 cells were seeded in a 96-well plate (Corning) at a density of 1.3×10^4 cells/well and incubated overnight. After which, 48 wells of JEG-3 cells were infected with ZIKV at a MOI of 5, while the other 48 wells were mock-infected with DMEM medium with 2% FCS for 1 h at 37 °C, 5% CO_2. The cells were then washed twice with 1 X PBS and

incubated in DMEM medium with 2% FCS overnight at 37 °C, 5% CO_2. After the cells were fixed, indirect immunofluorescence assay was performed and the percentage infection of each well was determined using the same methods described above. Finally, the Z-factor was calculated using the formula: $1 - \frac{3(\sigma_p + \sigma_n)}{|\mu_p - \mu_n|}$, where σ refers to the standard deviation, μ refers to the mean, p refers to the positive control (ZIKV-infected) and n refers to the negative control (mock).

Hits Validation The hits from the primary screen were validated using cell viability assays and post-treatment, dose-dependent viral plaque reduction assays. The cell viability profiles of the compounds were evaluated using the alamarBlue™ Cell Viability Reagent (ThermoFisher). Briefly, JEG-3 cells seeded in a 96-well plate (Corning) at a density of 1.3×10^4 cells/well were treated with the compounds at various concentrations and incubated overnight at 37 °C, 5% CO_2. After incubation, the media was removed and the cells were incubated with the alamarBlue™ Cell Viability Reagent (ThermoFisher) at 37 °C, 5% CO_2 for 2.5 h. Fluorescence readings were then taken using the Infinite™ 200 series microplate reader (Tecan) with an emission wavelength of 585 nm and excitation wavelength of 570 nm and the cell viabilities were determined. Triplicate readings were done for each concentration and the measurements of the drug-treated or 0.1% DMSO-treated cells were normalized against that of non-treated cells.

Dose-dependent viral plaque reduction assays were performed to validate the anti-ZIKV activity of the hits. JEG-3 cells were seeded in a 24-well plate (Greiner Bio-One) at a density of 7×10^4 cells/well and incubated overnight at 37 °C, 5% CO_2. The cells were then infected with ZIKV at a MOI of 5 for 1 h at 37 °C. After which, the cells were washed twice with 1 X PBS, before being treated with the required concentrations of drugs, with triplicates done per concentration. The plates were then incubated for 24 h at 37 °C, 5% CO_2. The supernatants were then harvested and plaque assays were done to determine the virus titres.

Viral Plaque Assays For the quantitation of virus titres, BHK-21 cells were first seeded in 24-well plates (Greiner Bio-One) at a density of 5×10^4 cells/well and incubated at 37 °C, 5% CO_2 overnight. The supernatants from virus-infected samples were subjected to 10-fold serial dilution using RPMI-1640 medium with 2% FCS. The seeded BHK-21 cells were then infected with 100 μL of the diluted virus inoculum and incubated at 37 °C, 5% CO_2 for 1 h, with gentle rocking every 15 min to ensure homogenous infection. After the incubation, the cells were washed twice with 1 X PBS, before being overlaid with RPMI-1640 medium containing 1% carboxymethyl-cellulose (CMC) and 2% FCS. The cells were then incubated for 4 days at 37 °C, 5% CO_2. After which, the cells were fixed and stained with 4% Paraformaldehyde (PFA) and 1% crystal violet. The virus titres were then calculated in plaque forming units (PFU) per milliliter.

Determining the CC_{50} and IC_{50} of Pinocembrin To determine the CC_{50} of pinocembrin, JEG-3 cells seeded in a 96-well plate (Corning) at a density of 1.3×10^4 cells/well were treated with pinocembrin at nine different concentrations, 0, 39.0, 78.0, 117, 156, 195, 234, 273 and 312 μM (equivalent to 0, 10, 20, 30, 40, 50, 60, 70 and 80 μg/ml). The cell viability at each concentration was then determined using the alamarBlue™ Cell Viability Reagent (ThermoFisher), following the same protocol as in 'Hits Validation'. The values were then fit into a non-linear regression curve and the CC_{50}, which is the concentration that results in 50% cell viability, was calculated using GraphPad Prism by interpolation. To determine the IC_{50} of pinocembrin, JEG-3 cells seeded in a 24-well plate (Greiner Bio-One) at a density of 7×10^4 cells/well were infected with ZIKV at a MOI of 5 for 1 h before being treated with pinocembrin at seven different concentrations, 0, 7.80, 39.0, 78.0, 117, 156 and 195 μM (equivalent to 0, 2, 10, 20, 30, 40 and 50 μg/ml). After 24 h incubation at 37 °C, 5% CO_2, the supernatants were then harvested and plaque assays were done to determine the virus titres. Similarly, the virus titres were fit into a non-linear regression curve and the IC_{50}, which is the concentration that results in 50% inhibitory effect, was then calculated using GraphPad Prism by interpolation.

Investigating the Anti-ZIKV Effect of Pinocembrin in Other Cell Lines BHK-21, Huh7 and HEK293T cells were seeded in separate 24-well plates (Greiner Bio-One) at a density of 6×10^4 cells/well, 9×10^4 cells/well and 1×10^5 cells/well respectively and incubated overnight at 37 °C, 5% CO_2. The cells were then infected with ZIKV at MOI of 5 for 1 h at 37 °C. After which, the cells were washed twice with 1 X PBS before being treated with 0.1% DMSO, 19.5 or 39.0 μM of pinocembrin. After incubation for 24 h at 37 °C, 5% CO_2, the supernatants were collected for quantitation of virus titres by plaque assays. The cell viability of pinocembrin was determined using the alamarBlue™ Cell Viability Reagent (ThermoFisher) as in 'Hits Validation'.

Time-of-Addition and Time-of-Removal Studies For both studies, JEG-3 cells were seeded in separate 96-well plates (Corning) at a density of 1.3×10^4 cells/well and incubated overnight at 37 °C, 5% CO_2. The cells were then infected with ZIKV at a MOI of 5 for 1 h at 37 °C. For the time-of-addition study, cells were washed twice with 1 x PBS before being incubated in DMEM medium with 2% FCS at 0 h post infection (hpi). Subsequently, at 0, 2, 4, 6, 8, 12, 18 and 24 hpi, the cells were treated with 156 μM of pinocembrin. For the time-of-removal study, cells were washed twice with 1 x PBS before being treated with 156 μM of pinocembrin at 0 hpi. The drug was then carefully aspirated and replaced with 100 μL of DMEM medium with 2% FCS at the same time points as the time-of-addition study. For both studies, cells treated with 0.1% DMSO were included as positive controls and all supernatants were harvested at 24 hpi for quantitation of virus titres by plaque assays.

Pre-treatment and Virus Inactivation Assays For the pre-treatment assay, JEG-3 cells seeded in a 24-well plate (Greiner Bio-One) at a density of 7×10^4 cells/well were treated with 156 μM of pinocembrin or 0.1% DMSO for 2 h at 37 °C, 5% CO_2 before being washed twice with 1 X PBS and infected with ZIKV at a MOI of 5 for 1 h. After which, the cells were again washed twice with 1 x PBS before being incubated in DMEM medium with 2% FCS for 24 h at 37 °C, 5% CO_2. The supernatants were then harvested for plaque assays. For the virus inactivation assay, ZIKV was treated with 156 μM of pinocembrin or 0.1% DMSO for 30 min at 37 °C, 5% CO_2. The viruses were then subjected to centrifugal filtration in 100,000-molecular-weight centrifugal filter units (Millipore, Darmstadt, Germany) at $1500 \times g$ for 5 min, 4 °C to remove the excess unbound drug. 1 ml of 1 X PBS was then added to the viruses and the viruses were subjected to another round of centrifugation using the same filter units. The purified viruses were then re-suspended in appropriate volumes of DMEM medium with 2% FCS to make up the original concentration of the virus. JEG-3 cells were then infected with these purified ZIKV for 1 h. After washing twice with 1 X PBS and incubation for 24 h, the supernatants were similarly harvested for quantitation of virus titres by plaque assays.

Quantitative Reverse Transcription-Polymerase Chain Reaction (qRT-PCR) For preparation of the samples for qRT-PCR, JEG-3 cells seeded in 24-well plates at a density of 7×10^4 cells/well were infected with ZIKV at a MOI of 5 or mock-infected with DMEM medium with 2% FCS for 1 h at 37 °C, 5% CO_2. After which, the cells were washed twice with 1 X PBS before being treated with 156 μM pinocembrin, 0.1% DMSO or DMEM medium with 2% FCS, which served as vehicle and positive controls respectively. At 8 and 14 hpi, total cellular RNA was extracted from all the samples, using the RNeasy Mini Kit (QIAGEN), according to the manufacturer's protocol.

Reverse transcription was first performed to generate the cDNA of either the positive-sense or negative-sense viral RNA. Samples were assayed in a 25 μL reaction mixture containing 5 μL of M-MLV 5X Reaction Buffer (Promega), 1 μL of dNTP mix, 1 μL of 200 units of M-MLV reverse transcriptase (Promega), 1 μL of either the forward or reverse primer (10 μM), 6 μl of RNA and 11 μL of nuclease-free water. The forward primer or the reverse primer was used to transcribe the cDNA of the negative-sense or positive-sense ZIKV RNA respectively.

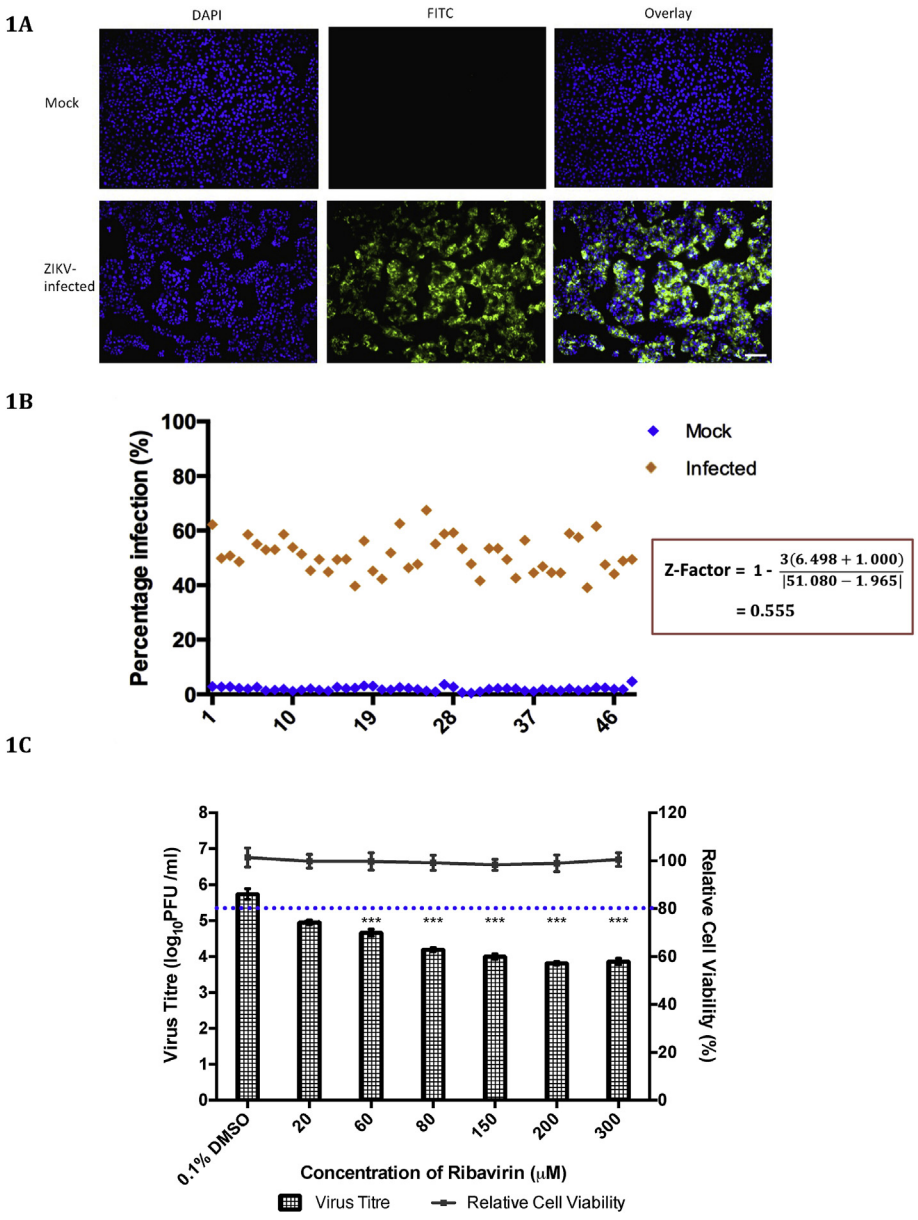

Fig. 1. Optimization of Z-Factor and positive control concentration for the primary screen. (A) Representative indirect immunofluorescence images of mock (media-treated) and ZIKV-infected JEG-3 cells (MOI 5) at 10× magnification. High levels of FITC signal, corresponding to ZIKV envelope protein, could be observed in the ZIKV-infected cells as compared to the mock, indicating the specificity of the primary antibody. The DAPI channel corresponds to live cell nuclei. Scale bar = 100 μm. (B) Graph showing a clear separation of infection rates between the mock and ZIKV-infected cells, yielding a Z-factor of 0.555, which indicates that the assay is an excellent one. (C) Ribavirin was able to inhibit ZIKV replication in a dose-dependent manner, while maintaining good cell viability. The concentration of ribavirin to be used as positive control for the primary screen was chosen to be 80 μM since it displayed significant inhibition of ZIKV infection (1.5 $\log_{10}$ decrease in virus titre) without being cytotoxic. The line graph for cell viability corresponds to the secondary axis. *** denotes p value < 0.001 using one-way ANOVA with Dunnett's post-test. Error bars represent the standard deviations of triplicate means.

Reverse transcription was then carried out for 30 min at 42 °C. After reverse transcription was completed, qPCR was conducted for second strand synthesis, amplification and quantification of the viral cDNA. The qPCR reaction was conducted in the Applied Biosystems StepOnePlus real-time PCR system (Applied Biosystems, Carlsbad, CA) in a 20 μL mixture containing 10 μL of PrimeTime® Gene Expression Master Mix (IDT), 0.5 μL each of the forward and reverse primers, 0.5 μL of the pan-ZIKV-1 probe, 1 μL of the cDNA and nuclease-free water. The reaction was performed with the following steps: polymerase activation at 94 °C for 2 min and 40 cycles of PCR (denaturation for 15 s at 94 °C and annealing and extension at 60 °C for 20 s). The primer sequences were as follows: forward, 5′-GAGTGTGATCCAGCCG TTATT-3'; reverse, 5′-CAGCCTCCATGTGTCATTCT-3'. The cycle threshold values obtained for the samples were normalized using β-actin gene as the endogenous control. The absolute ZIKV positive-sense and negative-sense viral RNA copy numbers were then derived from the cycle threshold values, by referencing against a standard curve.

SDS-PAGE and Western Blot Similar to the samples preparation for qRT-PCR, ZIKV-infected or mock-infected JEG-3 cells were treated with 156 μM of pinocembrin, 0.1% DMSO or DMEM medium with 2% FCS. The treated cells were incubated for 14 and 20 h at 37 °C, 5% CO_2. After incubation, cells were lysed by adding 100 μL of 1 X Laemmli SDS-PAGE buffer for 10 min before scraping down the cell lysate. Before SDS-PAGE was performed, the samples were boiled at 100 °C for 10 min. The samples were then separated with 10% acrylamide gels ran at 100 V for 2.5 h, using the PageRuler prestained protein ladder (Fermentas) as a standard. Subsequently, the separated proteins on the gel were transferred to a nitrocellulose membrane via the Bio-Rad semidry transfer system (Bio-Rad) at 1.3 A for 10 min.

For detection of the ZIKV envelope protein, the membrane was first blocked with 5% skim milk dissolved in Tris-buffered saline-Tween 20 (TBST) for 1 h. After washing thrice with TBST, the membrane was incubated with the 1° antibody, ZIKV anti-E-protein DIII ZV-67 (Absolute Antibody) for 1 h. The membrane was then washed thrice with TBST followed by incubation with the polyclonal goat anti-rabbit IgG (H + L) horseradish peroxidase 2° antibody (Thermo Scientific) for 1 h. After which, the membrane was again washed thrice with TBST and developed via the enhanced chemiluminescence (ECL) method using the SuperSignal West Pico chemiluminescent substrate (Thermo Scientific).

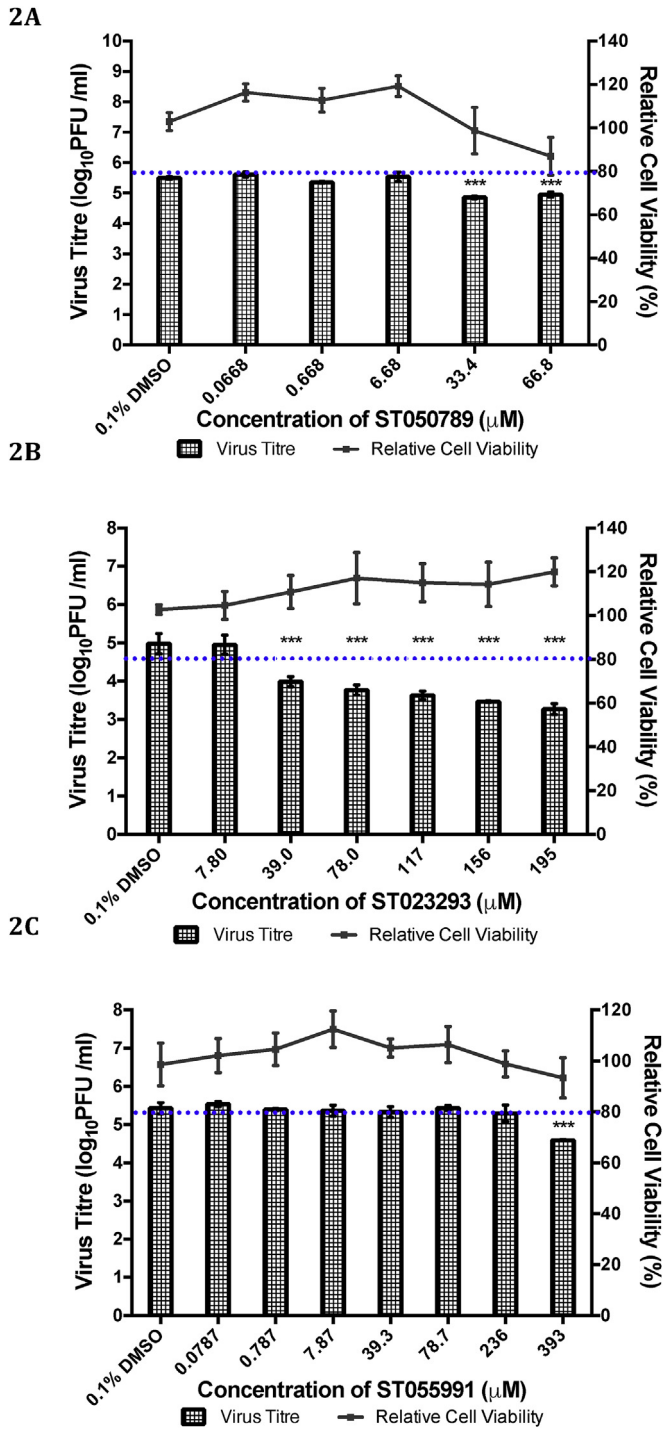

Fig. 2. Dose-dependent study of anti-ZIKV effects of selected hits observed by plaque assays. (A) Treatment of ZIKV-infected JEG-3 cells (MOI 5) with 33.4 μM of ST050789 (equivalent to 10 μg/ml) resulted in a 0.6 $\log_{10}$ decrease in virus titre but this inhibitory effect plateaus at 66.8 μM (equivalent to 20 μg/ml, the screening concentration). (B) Treatment of ZIKV-infected JEG-3 cells (MOI 5) with ST023293 resulted in significant dose-dependent decrease in virus titre, with a 1.7 $\log_{10}$ decrease at 195 μM (equivalent to 50 μg/ml), without being cytotoxic. (C) ST055991 did not appear to have any significant anti-ZIKV effect, except at 393 μM (equivalent to 100 μg/ml). The line graph for cell viability corresponds to the secondary axis. *** denotes p value < 0.001 using one-way ANOVA with Dunnett's post-test. Error bars represent standard deviations of triplicate means.

Antiviral Activity against Other Viruses The antiviral effect of pinocembrin was further investigated against DENV2, CHIKV and EV-A71. Cell viability assays were first carried out on Huh7, HeLa and RD cells to find out the concentration range at which pinocembrin is non-cytotoxic. This was carried out using the alamarBlue™ Cell Viability Reagent (ThermoFisher), following the same protocol as in 'Hits Validation'. Dose-dependent viral plaque reduction assays were then performed to determine if pinocembrin is effective in inhibiting viral replication. The table below shows the cell line, seeding density on a 24 well plate, MOI and incubation time used for the assays against the three viruses. Similar to 'Hits Validation', the supernatants are harvested for virus quantitation by plaque assays after the incubation time.

Virus	Cell Line	Seeding Density/per well	MOI	Incubation Time/hours
DENV2	Huh7	7×10^4	1	48
CHIKV	HeLa	9×10^4	1	48
EV-A71	RD	1×10^5	1	12

Statistical Analyses One-way analysis of variance (ANOVA) tests were performed for all drug treatment experiments to determine the significance of the results. Dunnett's post-tests were further conducted for samples that displayed statistical significance (p value < 0.05) from the ANOVA analysis, where the data of the treated samples were compared against that of the vehicle (0.1% DMSO-treated) controls. Results from the tests were used to evaluate if treatment with the concentrations of compounds resulted in statistically significant difference as compared to the vehicle controls.

3. Results

Development of the Immunofluorescence-based Screening Assay Prior to the actual screen on the flavonoid derivatives library, a few parameters were optimized to ensure that the immunofluorescence-based screening assay is suitable and reliable for the identification of potential ZIKV inhibitors. Firstly, the Z-factor, a statistical parameter that assesses assay robustness, was determined. 48 wells of JEG-3 cells were infected with ZIKV at a MOI of 5 while the other 48 wells were mock-infected with DMEM medium with 2% FCS. Indirect immunofluorescence assay was then performed and the infection rate of each well determined. As shown in Fig. 1A, strong FITC signals, corresponding to ZIKV envelope protein, were detected in ZIKV-infected wells, while no signal was observed in mock-infected wells. This indicates the specificity of the primary antibody. A clear separation between the infection rates of the mock and ZIKV-infected wells was also observed, yielding a Z-factor of 0.555 (Fig. 1B). This value indicates that the assay is an excellent one and is sufficiently robust for the screening of ZIKV inhibitors (Zhang et al., 1999).

To ensure the reliability of the assay, a positive control was also included in the primary screen. Ribavirin was selected as the positive control as it has been shown to inhibit ZIKV replication *in vitro* and to reduce viremia in ZIKV-infected mice (Kamiyama et al., 2017). As shown in Fig. 1C, ribavirin exhibited significant dose-dependent inhibition of ZIKV infection in JEG-3 cells infected with ZIKV at MOI 5, as compared to the 0.1% DMSO-treated control. Furthermore, good cell viability was maintained for all the concentrations tested. This suggests that the antiviral effects displayed were not attributed to drug-induced cell death. 80 μM (equivalent to 20 μg/ml), was chosen as the optimal concentration for the primary screen since it displayed significant inhibition of ZIKV infection (1.5 $\log_{10}$ decrease in virus titre) without being cytotoxic.

Primary Screen of ZIKV-infected JEG-3 Cells against Flavonoid Derivatives Library After the immunofluorescence-based screening assay has been established, a primary screen was conducted on a library of 483 flavonoid derivatives to identify potential anti-ZIKV compounds.

Compounds were screened at a final concentration of 20 μg/ml and the percentage inhibition of ZIKV replication of each compound, as compared to 0.1% DMSO control, was determined. Compounds that displayed ≥50% inhibition of ZIKV replication were arbitrarily classified as hits (Table S1).

ST023293 is a potent inhibitor of ZIKV replication From the 16 hits identified, three compounds were selected for further evaluation of their antiviral properties. Their compound IDs are ST050789, ST023293 and ST055991. These compounds were chosen after comparing their nuclei counts against that of the 0.1% DMSO-treated vehicle controls and manually checking all 16 wells under the microscope, to eliminate compounds that are potentially cytotoxic (Fig. S1). The compounds were also selected due to their novelty and these details, in addition to their molecular structures, can be found in Table S2.

The anti-ZIKV activities of these compounds were validated by conducting dose-dependent, post-treatment viral plaque reduction assays in ZIKV-infected JEG-3 cells. In addition, cell viability assays were conducted to ensure that the anti-ZIKV effect displayed by the compounds were not due to cell cytotoxicity.

As shown in Fig. 2, ST050789 caused a 0.6 $\log_{10}$ decrease in virus titre at 33.4 μM (equivalent to 10 μg/ml), but this inhibitory effect seemed to plateau at 66.8 μM (equivalent to 20 μg/ml, the screening concentration). Higher concentrations of the drug were also found to be cytotoxic (Fig. 2A). On the other hand, ST023293 caused a 1 $\log_{10}$ decrease in virus titre at 39.0 μM (equivalent to 10 μg/ml) and showed dose-dependent ZIKV inhibition at non-cytotoxic concentrations of 39.0 μM to 195 μM (equivalent to 50 μg/ml), displaying a 1.7 $\log_{10}$ decrease in virus titre at 195 μM (Fig. 2B). ST055991 did not show any significant inhibition, except at 393 μM (equivalent to 100 μg/ml), indicating that it was most likely a false positive hit (Fig. 2C). As such, since ST023293 displayed the strongest inhibitory effect among these three hits, ST023293 or pinocembrin was chosen as the lead compound for downstream studies.

Determining the CC_{50} and IC_{50} of pinocembrin and investigating its anti-ZIKV effect at different MOIs and in different cell lines Next, the CC_{50} and IC_{50} of pinocembrin against ZIKV were determined. Briefly, to determine the CC_{50} of pinocembrin, JEG-3 cells were treated with nine different concentrations of pinocembrin and the cell viability for each concentration was determined. Conversely, to determine the IC_{50} of pinocembrin, ZIKV-infected JEG-3 cells (MOI 5) were treated with seven different concentrations of pinocembrin and the virus titres were determined via plaque assays. The cell viability values and virus titres were then fit into non-linear regression curves, as shown in Fig. 3A and B respectively. The CC_{50} of pinocembrin, which is the concentration that results in 50% cell viability, was determined to be 251 μM while its IC_{50}, which is the concentration that results in 50% inhibitory effect, was determined to be 17.4 μM.

The anti-ZIKV effect of pinocembrin was also investigated in JEG-3 cells infected with ZIKV at different MOIs. 0.1% DMSO-treated cells were included as positive controls. As shown in Fig. 3C, the virus titres in the positive controls increased correspondingly with an increase in MOI, indicating that the experiment was properly carried out. Treatment of ZIKV-infected JEG-3 cells with 156 μM (equivalent to 40 μg/ml) pinocembrin resulted in strong inhibition of ZIKV infection at all MOIs, with a greater decrease in virus titre observed with increasing MOIs. Treatment with pinocembrin resulted in the strongest inhibition at MOI 5, with a 2.2 $\log_{10}$ decrease in virus titre.

The anti-ZIKV effect of pinocembrin was further investigated in other ZIKV-permissible cell lines, namely BHK-21, Huh7 and HEK293T cells (Chan et al., 2016). The ZIKV-infected cells were treated with pinocembrin at 19.5 or 39.0 μM, as these concentrations were found to be non-cytotoxic across all three cell lines. As shown in Fig. 3D and F, pinocembrin did not result in significant inhibition of ZIKV infection in infected BHK-21 and HEK293T cells. On the other hand, significant inhibitory effect by pinocembrin was observed in ZIKV-infected Huh7 cells, with a 1.1 $\log_{10}$ decrease in virus titre observed upon treatment with 39.0 μM pinocembrin (Fig. 3E). This difference in susceptibility to pinocembrin treatment may be due to the specific mechanism of action of the drug. Collectively, we have shown that pinocembrin caused significant inhibition against ZIKV in JEG-3 cells infected with ZIKV at all MOIs, with the greatest inhibitory effect observed at MOI 5. Pinocembrin was also effective in inhibiting ZIKV in another physiologically relevant cell line, Huh7, but not in BHK-21 and HEK293T, suggesting some specificity in its mechanism of action (Van Der Hoek et al., 2017).

Time-of-Addition and Time-of-Removal Studies of Pinocembrin in ZIKV infection To determine the window in the ZIKV replication cycle when pinocembrin acts on, time-of-addition and time-of-removal studies were performed. For time-of-addition studies, ZIKV-infected JEG-3 cells were treated with 156 μM pinocembrin at different timepoints (0, 2 4, 6, 8, 12, 18, 24 hpi). On the other hand, for time-of-removal studies, the ZIKV-infected cells were treated with 156 μM pinocembrin at 0 hpi and drug was subsequently removed and replaced with DMEM medium with 2% FCS at different time points. For both studies, ZIKV-infected, 0.1% DMSO-treated cells were included as positive controls for each timepoint (Fig. 4C). All supernatants were then harvested at 24 hpi for virus titre determination using plaque assays (Fig. 4A).

Fig. 4B shows the graph displaying the virus titres of ZIKV-infected, pinocembrin-treated cells from the time-of-addition and time-of-removal studies. As seen from the time-of-addition studies, a significant increase in virus titre was observed when the drug was added 18 hpi, as compared to 12hpi. Correspondingly, a sharp drop in virus titre was observed for the time-of-removal studies when the drug was removed 18 hpi, instead of 12 hpi. As such, this resulted in an interception point between the time-of-addition and time-of-removal graphs at around 16hpi. These results indicate that pinocembrin most likely acts on post-entry process(es) of the ZIKV replication cycle.

Pre-treatment and virus inactivation assays further confirmed that pinocembrin does not act on ZIKV binding and entry processes Pre-treatment and virus inactivation assays were also conducted to further confirm that pinocembrin does not act at an early stage of the ZIKV replication cycle. Specifically, the pre-treatment assay serves to determine if the drug interacts with host cell receptors to prevent virus binding and entry, by treating JEG-3 cells with 156 μM pinocembrin for 2 h prior to ZIKV infection. Conversely, the virus inactivation assay serves to investigate if the drug induces the disassembly of viral particles or interacts with viral surface proteins to interfere with its infectivity. ZIKV was first treated with 156 μM pinocembrin for 30 min at 37 °C, subjected to centrifugal filtration to remove the excess drug, before being used to infect the JEG-3 cells.

As seen in Fig. 5A and B, minimal inhibitory effect was observed for treated cells, as compared to the vehicle control (0.1% DMSO-treated) cells in both assays. Therefore, these serve to confirm that pinocembrin does not inhibit the ZIKV binding and entry process.

Pinocembrin inhibits ZIKV RNA Synthesis and ZIKV Protein Synthesis Subsequently, to evaluate the effect of pinocembrin on viral RNA synthesis, qRT-PCR was carried out on ZIKV-infected JEG-3 cells treated with 156 μM pinocembrin for 8 hpi and 14 hpi. Viral RNA was also quantitated for ZIKV-infected cells treated with 0.1% DMSO and DMEM medium with 2% FCS, which served as vehicle control and positive control respectively. The viral RNA cycle threshold values of all samples obtained were normalized with β-actin, before being converted to copy numbers using the standard curve as reference. Based on the qRT-PCR results, treatment with 156 μM pinocembrin resulted in a significant decrease in both positive- and negative-sense ZIKV RNA at both time points (Fig. 6A and B). This suggests that pinocembrin attenuates ZIKV viral RNA synthesis.

Western blot was performed to determine the effect of pinocembrin on viral protein synthesis, specifically that of the ZIKV envelope protein. Uninfected cells treated with media, 0.1% DMSO and 156 μM pinocembrin for 20 hpi were included as negative controls and infected cells with media were included for both time points (14 hpi and 20 hpi)

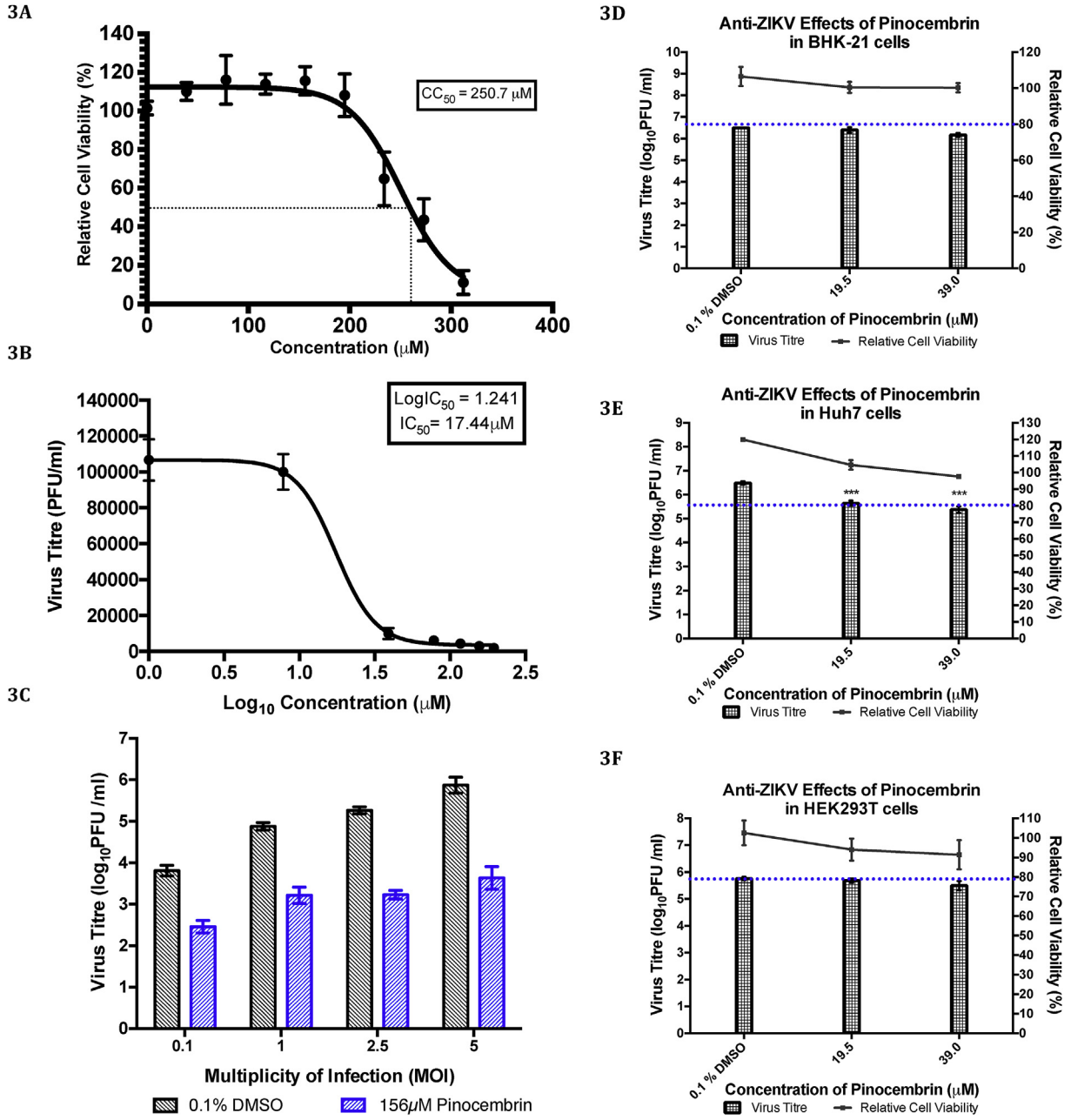

Fig. 3. CC_{50}, IC_{50} and anti-ZIKV effect of pinocembrin at different MOIs and in different cell lines. (A) Nine concentration values were tested for cytotoxicity in JEG-3 cells using Alamarblue assay and the cell viability values were then fit into a non-linear regression curve. The CC_{50}, which is the concentration that results in 50% cell viability, was then calculated using GraphPad Prism by interpolation. The CC_{50} of pinocembrin was determined to be 250.7 μM. (B) The inhibitory effect of pinocembrin at 7 concentration values in ZIKV-infected JEG-3 cells (MOI 5) were determined and the virus titres were fit into a non-linear regression curve. The IC_{50}, which is the concentration that results in 50% inhibitory effect, was then calculated using GraphPad Prism by interpolation. The IC_{50} of pinocembrin was determined to be 17.44 μM. (C) Treatment of JEG-3 cells, infected with ZIKV at different MOIs, 0.1, 1, 2.5 and 5, with 156 μM pinocembrin (equivalent to 40 μg/ml) was shown to cause strong inhibition against ZIKV infection, as compared to the vehicle controls (0.1% DMSO-treated cells). At MOI 0.1, treatment with pinocembrin resulted in 1.4 $\log_{10}$ decrease in virus titre while at MOI 5, treatment with pinocembrin resulted in the strongest inhibition, with 2.2 $\log_{10}$ decrease in virus titre. (D) Treatment of ZIKV-infected BHK-21 cells (MOI 5) with pinocembrin did not result in significant inhibition of ZIKV infection. (E) Treatment of ZIKV-infected Huh7 cells (MOI 5) with pinocembrin resulted in significant inhibition of ZIKV infection. Treatment with 19.5 μM pinocembrin resulted in 0.85 $\log_{10}$ decrease in virus titre while treatment with 39.0 μM pinocembrin resulted in 1.1 $\log_{10}$ decrease in virus titre. (F) Treatment of ZIKV-infected HEK293T cells (MOI 5) with pinocembrin did not result in significant inhibition of ZIKV infection. *** denotes p value $<$ 0.001 using one-way ANOVA with Dunnett's post-test. Error bars represent standard deviations of triplicate means.

to ensure that the 0.1% DMSO did not affect viral protein expression. β-actin served as the loading control in the experiment and also helped to ensure that treatment of cells with pinocembrin did not affect the production of host cellular proteins. As shown in Fig. 6C and D, treatment of cells with 156 μM pinocembrin for both 14hpi and 20hpi resulted in significant reduction in ZIKV envelope protein detected, as compared to the ZIKV-infected, 0.1% DMSO-treated cells. This suggests that pinocembrin inhibits ZIKV protein production, which can explain the decrease in virus titres observed in plaque assays.

Pinocembrin demonstrates broad-spectrum antiviral effects against DENV2 and CHIKV To investigate the possible broad spectrum effects of pinocembrin, the antiviral activity of pinocembrin against

4A

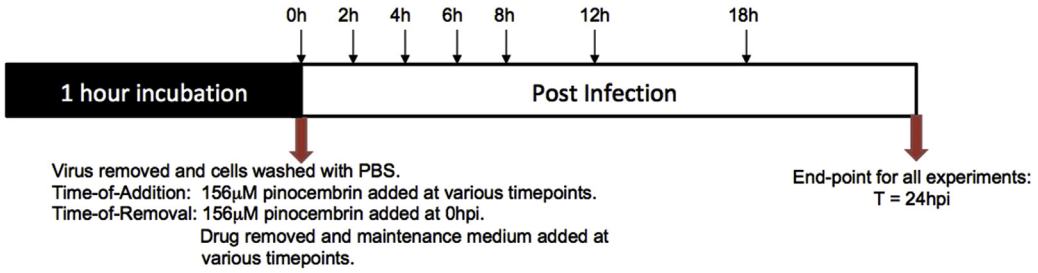

4B

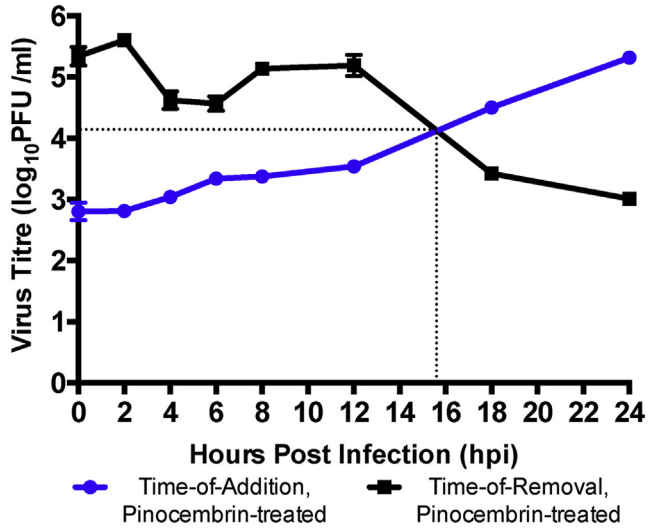

4C

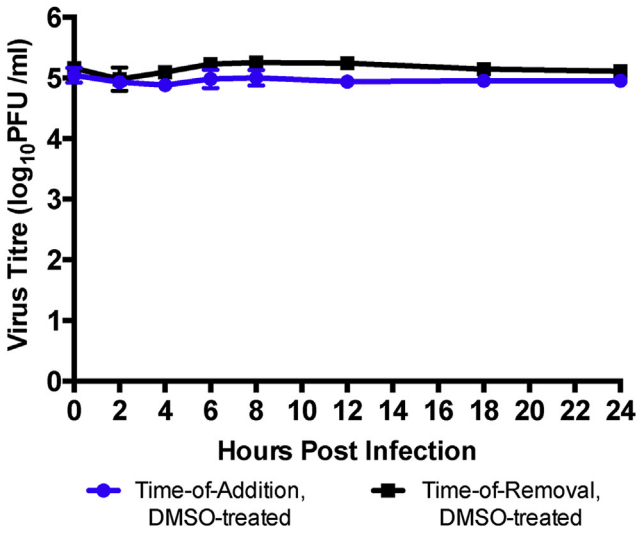

Fig. 4. Pinocembrin acts on postentry processes of the ZIKV replication cycle. (A) Schematic diagram describing the workflow for the time-of-addition and time-of-removal studies. JEG-3 cells were infected with ZIKV at MOI 5 for 1 h. 156 μM pinocembrin was then added or removed at different timepoints post-infection in the time-of-addition and time-of-removal studies respectively. All supernatants were harvested for plaque assays at 24 hpi for virus titre determination. (B) Graph displaying the ZIKV virus titres from the time-of-addition and time-of-removal studies. The interception point is observed to be at around 16 hpi. This suggests that pinocembrin was acting on postentry process(es) of the ZIKV replication cycle. (C) ZIKV-infected cells (MOI 5) treated with 0.1% DMSO were included as positive controls for both the time-of-addition and time-of-removal studies.

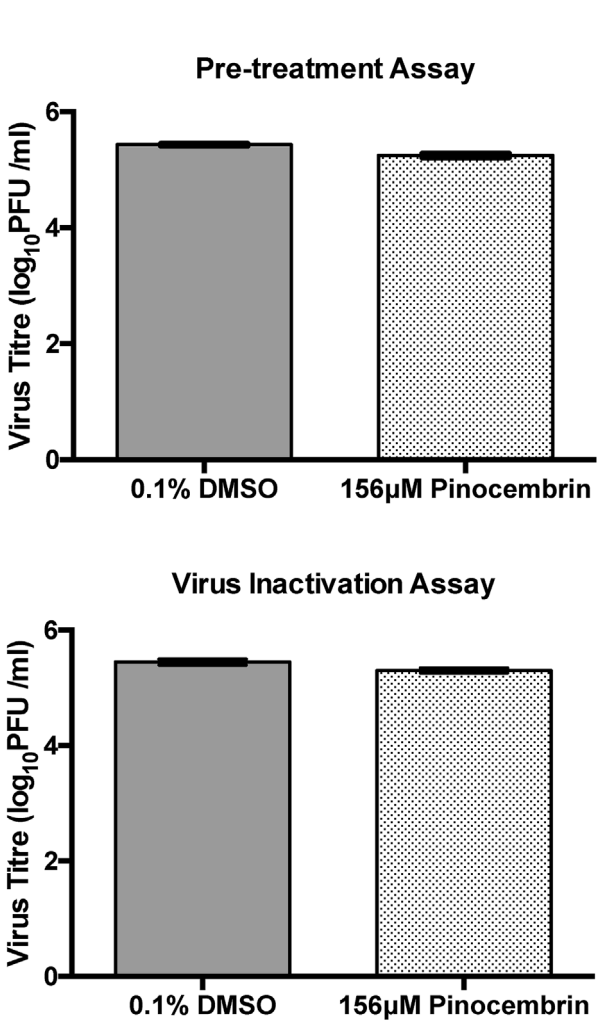

Fig. 5. Pinocembrin does not inhibit ZIKV binding and entry processes. (A) Pre-treatment of cells with 156 μM pinocembrin prior to ZIKV infection at MOI 5 resulted in minimal inhibitory effect. This indicates that pinocembrin does not interact with host cell receptors to inhibit ZIKV infection. (B) Co-treatment of ZIKV with 156 μM pinocembrin also failed to cause a significant inhibition of ZIKV infection. This indicates that pinocembrin does not interact with virus surface proteins or induce lysis of viral particles to inhibit ZIKV infection.

DENV2, CHIKV and EV-A71 were studied. Out of the three viruses, pinocembrin was shown to inhibit DENV2 and CHIKV replication at non-cytotoxic concentrations. As shown in Fig. 7A and B, treatment of DENV2-infected Huh7 cells with 39.0 μM pinocembrin resulted in 0.71 $\log_{10}$ decrease in virus titre while treatment of CHIKV-infected HeLa cells with 21.5 μM pinocembrin resulted in 1.05 $\log_{10}$ decrease in virus titre. Treatment of EV-A71-infected RD cells with pinocembrin, on the other hand, did not show any significant inhibitory effect (Fig. 7C).

4. Discussion

The potential for ZIKV to cause another outbreak and the severe neurological complications associated with its infection highlight the urgent need for effective antivirals against ZIKV. To address the current lack of approved antivirals for ZIKV infection, an immunofluorescence-based HTS platform using human placental JEG-3 cells was developed to screen for novel anti-ZIKV compounds. This screening assay was statistically validated to be sufficiently robust for hits identification, with a Z-factor of 0.555. The Z-factor is a simple and dimensionless parameter that ensures that the assay has sufficient dynamic range and limited data variability in order to identify hits with high fidelity (Zhang et al., 1999).

The immunofluorescence-based screening platform was subsequently used to screen a library of 483 flavonoid derivatives for inhibitory activity against ZIKV. Flavonoids are natural polyphenolic compounds commonly found in many fruits and vegetables. Historically, these natural compounds have been an important source of new drugs as they provide a diversity of chemical structures that can target various important proteins (Kumar and Pandey, 2013). Several flavonoids have been demonstrated to have anti-flaviviral effects, such as quercetin and fisetin, which are able to inhibit DENV2 replication in Vero cells, and baicalein against the Japanese encephalitis virus (JEV) (Johari et al., 2012; Zandi et al., 2011a, b). This study represented the first HTS assay that was done on the flavonoid derivatives library to identify anti-ZIKV compounds.

The primary screen on the 483 flavonoid derivatives identified 16 hits with ≥50% inhibition of ZIKV infection. Three hits, ST050789, ST023293 and ST055991, were further selected for validation due to the promising cell viabilities they exhibit and academic novelty. Among these three drugs, ST023293 displayed the strongest inhibition of ZIKV infection at non-cytotoxic concentrations. As such, ST023293 or pinocembrin was chosen as the lead compound for downstream studies.

Pinocembrin (5,7-dihydroxyflavanone) is one of the main flavonoids found in a wide array of plants including *Pinus* heartwood and *Eucalyptus* (Rasul et al., 2013). Being a natural plant-derived compound, it is also ubiquitous in everyday edible products such as honey, propolis, ginger roots, tea and red wine. Pinocembrin has been shown to have a wide range of pharmacological uses: antibacterial, anti-inflammatory, antifungal and anticancer (Rasul et al., 2013). Furthermore, it has also demonstrated neuroprotective effects in mouse or rat models for ischemic stroke, Alzheimer's disease and Parkinson's disease (Liu et al., 2014; Ma et al., 2018; Wang et al., 2014). Due to the promising results pinocembrin displayed in *in vitro* and *in vivo* studies, pinocembrin was approved in 2008 by the State Food and Drug Administration of China for clinical trials in patients with ischemic stroke and phase II clinical trials began in 2014 (Lan et al., 2016).

The antiviral activity of pinocembrin, however, remains poorly studied. To further validate the anti-ZIKV effect of pinocembrin in JEG-3 cells, the CC_{50} and IC_{50} of pinocembrin were determined to be 251 μM and 17.4 μM respectively, yielding a selectivity index (SI = CC_{50}/IC_{50}) of 14.4. The anti-ZIKV effect of pinocembrin was further investigated in other ZIKV-permissible cell lines and was found to be effective in inhibiting ZIKV in human hepatoma Huh7 cell line, but not baby hamster kidney BHK-21 and human embryonic kidney HEK293T cells. The human placental JEG-3 and human hepatoma Huh7 cell lines represent physiologically relevant cell lines that can be used to represent *in vitro* the trans-placental transmission and possible liver damage associated with ZIKV infection (Chan et al., 2016; Wu et al., 2017). Therefore, it will be worthwhile to investigate the specific mechanism of action of pinocembrin in inhibiting ZIKV infection to ameliorate these effects of ZIKV pathogenesis.

To elucidate the mechanism of action of pinocembrin in inhibiting ZIKV infection, time-of-addition and time-of-removal studies were performed on ZIKV-infected JEG-3 cells to determine the window in the ZIKV replication cycle when pinocembrin exerts its antiviral effect. The approximate timepoint at which the drug acts was observed to be at around 16 hpi, which indicates that pinocembrin acts on post-entry process(es) of the ZIKV replication cycle. Results from the pre-treatment and virus inactivation assays further confirmed that pinocembrin does not act on early steps of the ZIKV replication cycle, specifically the binding and entry steps. The lack of inhibitory effect when ZIKV was incubated with pinocembrin for 30 min at 37 °C in the virus inactivation assay also showed that pinocembrin does not cause disassembly of viral particles or affect their infectivity. Next, data from the qRT-PCR and Western Blot showed that pinocembrin attenuated synthesis of both positive- and negative-sense viral RNA and also inhibited the synthesis of the envelope protein in ZIKV-infected cells. Cumulatively, these

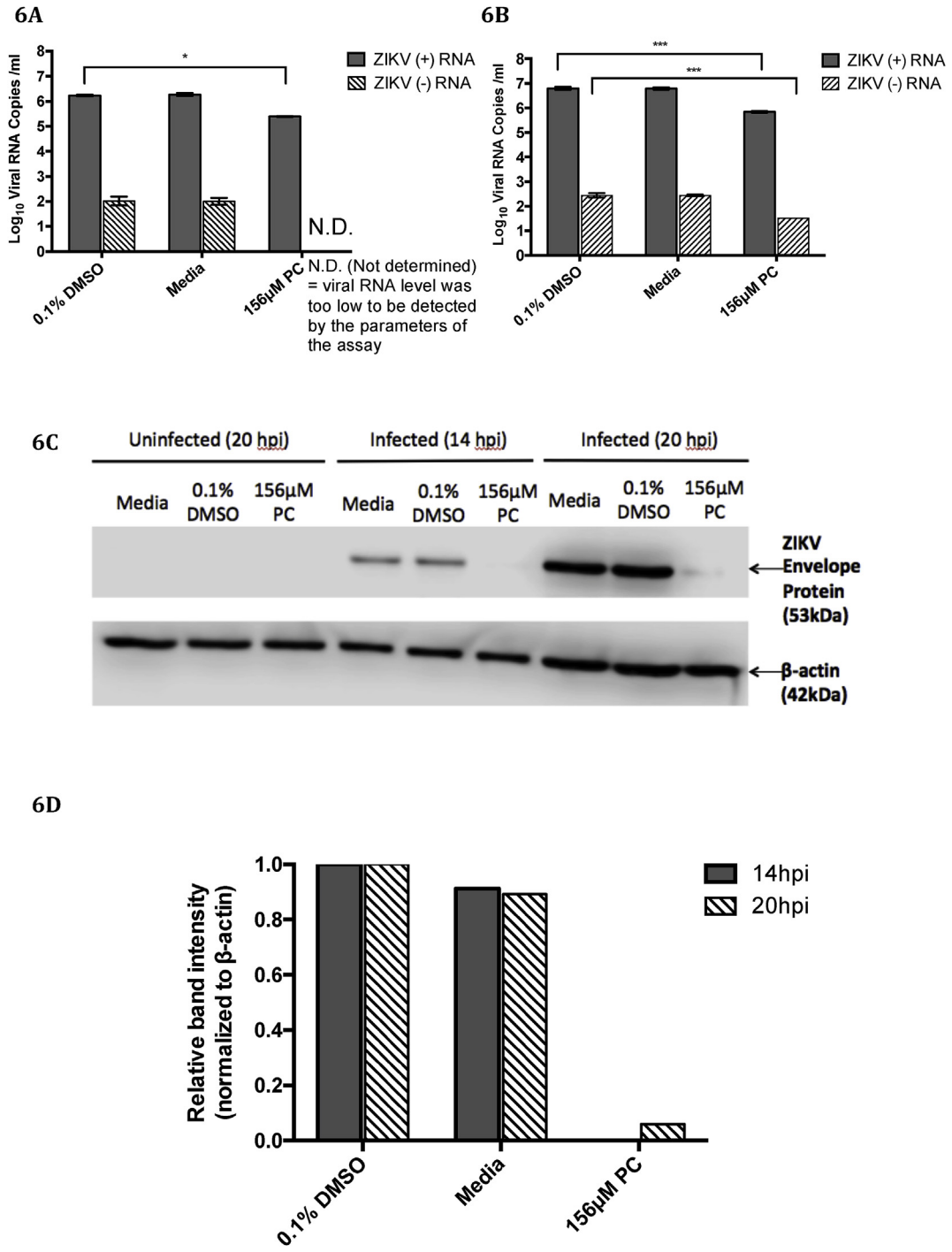

Fig. 6. Pinocembrin attenuates both ZIKV RNA and protein synthesis. qRT-PCR results show that treatment of ZIKV-infected JEG-3 cells (MOI 5) with 156 μM pinocembrin for both 8 hpi (A) and 14 hpi (B) resulted in a significant decrease in positive- and negative-sense ZIKV RNA production, as compared to the vehicle control (0.1% DMSO-treated) cells. * and *** denotes p values $<$ 0.1 and 0.001 respectively using one-way ANOVA with Dunnett's post-test. Error bars represent standard deviations of triplicate means. (C) Western blot analysis show that treatment of ZIKV-infected JEG-3 cells (MOI 5) with 156 μM pinocembrin for both 14 hpi and 20 hpi resulted in signficant reduction in ZIKV envelope protein production, as compared to the vehicle control (0.1% DMSO-treated) cells. (D) Graph showing the relative band intensities of drug-treated cells in relation to the vehicle control cells. PC, Pinocembrin.

results indicate that pinocembrin acts on post-entry process(es) of the ZIKV replication cycle.

We also attempted to select for a resistant mutant to determine if pinocembrin acts by targeting a viral factor or a host factor that can readily lead to escape mutants. This was done by serially passaging ZIKV in JEG-3 cells treated with gradually increasing concentrations of pinocembrin. JEG-3 cells were first infected with ZIKV at MOI 3 for 1 h before being treated with 19.5 μM pinocembrin which is close to the IC_{50} of pinocembrin (17.4 μM). After 48 h incubation, the supernatant was harvested and 200 μL of this virus inoculum was used for infection for the next passage while the rest was used for plaque assay to determine the virus titre. Pinocembrin treatment was increased by 19.5 μM at every passage until 156 μM. Our results showed that after 9 passages, the viruses still remained susceptible to pinocembrin treatment (Figure S2). This may suggest that instead of targeting a viral factor or a host factor that can readily lead to escape mutants,

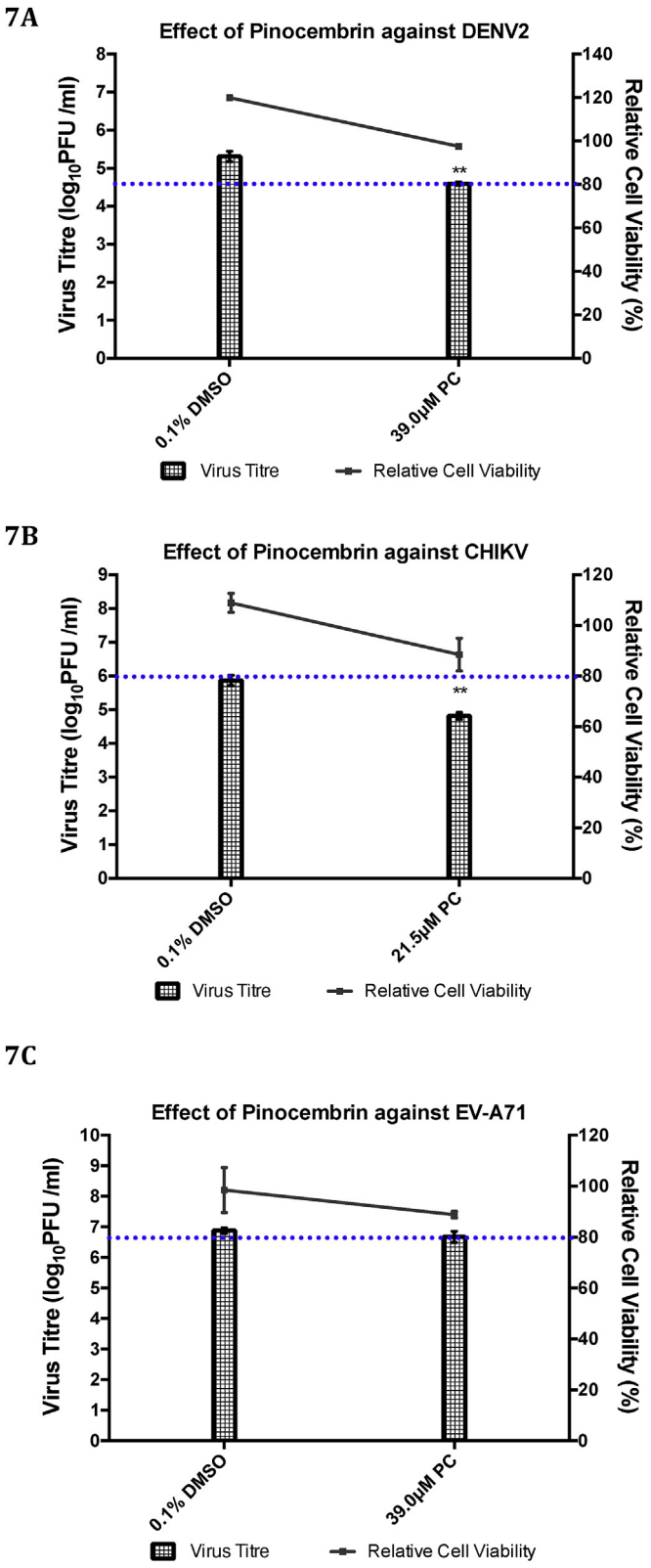

Fig. 7. Broad-spectrum effect of pinocembrin against other viruses. (A) Treatment of DENV2-infected Huh7 cells (MOI 1) with 39.0 μM pinocembrin resulted in 0.71 $\log_{10}$ decrease in virus titre. (B) Treatment of CHIKV-infected HeLa cells (MOI 1) with 21.5 μM pinocembrin resulted in 1.05 $\log_{10}$ decrease in virus titre. (C) Treatment of EV-A71-infected RD cells (MOI 1) with 39.0 μM pinocembrin did not have any significant inhibitory effect. ** denotes p value < 0.01 using one-way ANOVA with Dunnett's post-test. Error bars represent standard deviations of triplicate means. PC, Pinocembrin.

pinocembrin may act on host factors that are more resistant to the generation of escape viral mutants. Traditionally, host-targeting antivirals may be advantageous over direct-acting antivirals as they have a lower risk of viruses developing drug resistance via mutations to their genome, a phenomenon commonly observed in RNA viruses (Saiz and Martín-Acebes, 2017). Nevertheless, more detailed mechanism studies are imperative to determine the exact mechanism of action of pinocembrin.

The broad-spectrum antiviral effects of pinocembrin were also investigated. Out of the three viruses tested (DENV2, CHIKV and EV-A71), pinocembrin demonstrated significant inhibitory effect against DENV2 and CHIKV. DENV2 is closely related to ZIKV, belonging to the same genus *Flavivirus* and family *Flaviviridae* while CHIKV belongs to the *Alphavirus* of the *Togaviridae* family. All three viruses (ZIKV, DENV2 and CHIKV) are arthropod-borne viruses that share the same transmission vectors: *Aedes albopictus* and *Aedes aegypti* mosquitoes and have single-stranded positive-sense RNA genome (Lu et al., 2012). Due to their overlapping endemic regions and similar seasonal correlations, co-infections of these arboviruses have been increasingly recognized as a pertinent challenge (Rothan et al., 2018). Therefore, the preliminary results from this study may point to the potential development of pinocembrin as an effective broad-spectrum antiviral against these arboviruses.

In conclusion, this study has established a robust phenotype-based HTS platform, which was employed to screen a flavonoid derivatives library. Pinocembrin, a flavanone, was identified as a hit and was shown to display strong dose-dependent inhibition against ZIKV in the validation studies. Based on time course studies, the drug was shown to act on post-entry stage(s) of the ZIKV replication cycle. It also has significant inhibitory effects on ZIKV RNA and envelope protein production. While the exact mechanism of action of pinocembrin still remains to be studied, this study has revealed a novel use for pinocembrin as an antiviral candidate. In addition, this study has also discovered the potential use of pinocembrin as a broad-spectrum antiviral against other arboviruses. Nevertheless, since the results from this study were based on *in vitro* assays, downstream *in vivo* studies in relevant animal models will need to be carried out to assess the toxicity and efficacy of pinocembrin in an organism. Given that pinocembrin has been shown to have differential effects on different cell lines, where it was effective in inhibiting ZIKV replication in human placental and liver cells but not human embryonic kidney cells, it would be important to investigate the specific effects of pinocembrin in different tissues. Furthermore, as pinocembrin has been demonstrated to have anti-inflammatory and neuroprotective effects, it would be worthwhile to examine its effect on the systemic level, such as its ability to reduce ZIKV-induced symptoms like fever, rashes and to protect against ZIKV-related neurodegenerative effects (Lan et al., 2016). It is also important to note that a phase I clinical trial has been done on pinocembrin, which showed that pinocembrin did not cause any adverse effects and was tolerable up to 120 mg/day when administered intravenously to 58 healthy subjects (Cao et al., 2015). This indicates that pinocembrin is safe for administration as a drug, though its safety in pregnant women and children still needs to be evaluated.

Since the ZIKV outbreak in late 2014, many antiviral candidates have been shown to inhibit viral replication *in vitro* and some have been tested *in vivo*. However, there remains no effective ZIKV antiviral to date, indicating the difficulty in translating experimental results to the clinical setting (Saiz et al., 2018). Therefore, it is important for us to step up research in this area while carefully evaluating the safety and efficacy of the drug, in order to address the current lack of antivirals against ZIKV.

Acknowledgements

This work was supported by the NRF-NSFC Joint Research Grant NRF2016NRF-NSFC002-012.

Appendix A. Supplementary data

Supplementary data to this article can be found online at https://doi.org/10.1016/j.antiviral.2019.04.003.

References

Burke, R.M., Pandya, P., Nastouli, E., Gothard, P., 2016. Zika virus infection during pregnancy: what, where, and why? Br. J. Gen. Pract. 66, 122–123. https://doi.org/10.3399/bjgp16X683917.

Cao, G., Ying, P., Yan, B., Xue, W., Li, K., Shi, A., Sun, T., Yan, J., Hu, X., 2015. Pharmacokinetics, safety, and tolerability of single and multiple-doses of pinocembrin injection administered intravenously in healthy subjects. J. Ethnopharmacol. 168, 31–36. https://doi.org/10.1016/j.jep.2015.03.041.

Carpenter, A.E., Jones, T.R., Lamprecht, M.R., Clarke, C., Kang, I.H., Friman, O., Guertin, D.A., Chang, J.H., Lindquist, R.A., Moffat, J., Golland, P., Sabatini, D.M., 2006. CellProfiler: image analysis software for identifying and quantifying cell phenotypes. Genome Biol. 7. https://doi.org/10.1186/gb-2006-7-10-r100.

Cauchemez, S., Besnard, M., Bompard, P., Dub, T., Guillemette-Artur, P., Eyrolle-Guignot, D., Salje, H., Van Kerkhove, M.D., Abadie, V., Garel, C., Fontanet, A., Mallet, H.P., 2016. Association between Zika virus and microcephaly in French Polynesia, 2013-15: a retrospective study. Lancet 387, 2125–2132. https://doi.org/10.1016/S0140-6736(16)00651-6.

CDC C for D.C. and P, 2018. Areas with Risk of Zika. (WWW Document).

Chan, J.F.W., Yip, C.C.Y., Tsang, J.O.L., Tee, K.M., Cai, J.P., Chik, K.K.H., Zhu, Z., Chan, C.C.S., Choi, G.K.Y., Sridhar, S., Zhang, A.J., Lu, G., Chiu, K., Lo, A.C.Y., Tsao, S.W., Kok, K.H., Jin, D.Y., Chan, K.H., Yuen, K.Y., 2016. Differential cell line susceptibility to the emerging Zika virus: implications for disease pathogenesis, non-vector-borne human transmission and animal reservoirs. Emerg. Microb. Infect. 5, e93. https://doi.org/10.1038/emi.2016.99.

Cushnie, T.P.T., Lamb, A.J., 2011. Recent advances in understanding the antibacterial properties of flavonoids. Int. J. Antimicrob. Agents. https://doi.org/10.1016/j.ijantimicag.2011.02.014.

Dick, G.W.A., Kitchen, S.F., Haddow, A.J., 1952. Zika Virus (I). Isolations and serological specificity. Trans. R. Soc. Trop. Med. Hyg. 46, 509–520. https://doi.org/10.1016/0035-9203(52)90042-4.

Duffy, M.R., Chen, T.-H., Hancock, W.T., Powers, A.M., Kool, J.L., Lanciotti, R.S., Pretrick, M., Marfel, M., Holzbauer, S., Dubray, C., Guillaumot, L., Griggs, A., Bel, M., Lambert, A.J., Laven, J., Kosoy, O., Panella, A., Biggerstaff, B.J., Fischer, M., Hayes, E.B., 2009. Zika virus outbreak on Yap Island, Federated States of Micronesia. N. Engl. J. Med. 360, 2536–2543. https://doi.org/10.1056/NEJMoa0805715.

Fernandez-Garcia, M.D., Mazzon, M., Jacobs, M., Amara, A., 2009. Pathogenesis of flavivirus infections: using and abusing the host cell. Cell Host Microbe. https://doi.org/10.1016/j.chom.2009.04.001.

Gould, E., Solomon, T., 2008. Pathogenic flaviviruses. Lancet 371, 500–509. https://doi.org/10.1016/S0140-6736(08)60238-X.

Johari, J., Kianmehr, A., Mustafa, M.R., Abubakar, S., Zandi, K., 2012. Antiviral activity of baicalein and quercetin against the Japanese encephalitis virus. Int. J. Mol. Sci. 13, 16020–16045. https://doi.org/10.3390/ijms131216785.

Kamiyama, N., Soma, R., Hidano, S., Watanabe, K., Umekita, H., Fukuda, C., Noguchi, K., Gendo, Y., Ozaki, T., Sonoda, A., Sachi, N., Runtuwene, L.R., Miura, Y., Matsubara, E., Tajima, S., Takasaki, T., Eshita, Y., Kobayashi, T., 2017. Ribavirin inhibits Zika virus (ZIKV) replication in vitro and suppresses viremia in ZIKV-infected STAT1-deficient mice. Antivir. Res. 146, 1–11. https://doi.org/10.1016/j.antiviral.2017.08.007.

Kaul, T.N., Middleton, E., Ogra, P.L., 1985. Antiviral effect of flavonoids on human viruses. J. Med. Virol. 15, 71–79. https://doi.org/10.1002/jmv.1890150110.

Kleber de Oliveira, W., Cortez-Escalante, J., De Oliveira, W.T.G.H., do Carmo, G.M.I., Henriques, C.M.P., Coelho, G.E., Araújo de França, G.V., 2016. Increase in reported prevalence of microcephaly in infants born to women living in areas with confirmed zika virus transmission during the first trimester of pregnancy — Brazil, 2015. MMWR Morb. Mortal. Wkly. Rep. 65. https://doi.org/10.15585/mmwr.mm6509e2er.

Kumar, S., Pandey, A.K., 2013. Chemistry and biological activities of flavonoids: an overview. Sci. World J. https://doi.org/10.1155/2013/162750.

Kuno, G., Chang, G.J.J., 2007. Full-length sequencing and genomic characterization of Bagaza, Kedougou, and Zika viruses. Arch. Virol. 152, 687–696. https://doi.org/10.1007/s00705-006-0903-z.

Lan, X., Wang, W., Li, Q., Wang, J., 2016. The natural flavonoid pinocembrin: molecular targets and potential therapeutic applications. Mol. Neurobiol. https://doi.org/10.1007/s12035-015-9125-2.

Lei, J., Hansen, G., Nitsche, C., Klein, C.D., Zhang, L., Hilgenfeld, R., 2016. Crystal structure of zika virus ns2b-ns3 protease in complex with a boronate inhibitor. Science (80-.) 353, 503–505. https://doi.org/10.1126/science.aag2419.

Liu, R., Li, J. ze, Song, J. ke, Zhou, D., Huang, C., Bai, X. yu, Xie, T., Zhang, X., Li, Y.jie, Wu, C. xia, Zhang, L., Li, L., Zhang, T.tai, Du, G. hua, 2014. Pinocembrin improves cognition and protects the neurovascular unit in Alzheimer related deficits. Neurobiol. Aging 35, 1275–1285. https://doi.org/10.1016/j.neurobiolaging.2013.12.031.

Lu, X., Li, X., Mo, Z., Jin, F., Wang, B., Zhao, H., Shan, X., Shi, L., 2012. Rapid identification of chikungunya and dengue virus by a real-time reverse transcription-loop-mediated isothermal amplification method. Am. J. Trop. Med. Hyg. 87, 947–953. https://doi.org/10.4269/ajtmh.2012.11-0721.

Ma, Y., Li, L., Kong, L., Zhu, Z., Zhang, W., Song, J., Chang, J., Du, G., 2018. Pinocembrin protects blood-brain barrier function and expands the therapeutic time window for tissue-type plasminogen activator treatment in a rat thromboembolic stroke model. BioMed Res. Int 2018. https://doi.org/10.1155/2018/8943210.

Panche, A.N., Diwan, A.D., Chandra, S.R., 2016. Flavonoids: an overview. J. Nutr. Sci. https://doi.org/10.1017/jns.2016.41.

Rasul, A., Millimouno, F.M., Ali Eltayb, W., Ali, M., Li, J., Li, X., 2013. Pinocembrin: a novel natural compound with versatile pharmacological and biological activities. BioMed Res. Int 2013. https://doi.org/10.1155/2013/379850.

Rice-Evans, C., 2001. Flavonoid antioxidants. Curr. Med. Chem. 8, 797–807. https://doi.org/10.2174/0929867013373011.

Roby, J.A., Setoh, Y.X., Hall, R.A., Khromykh, A.A., 2015. Post-translational regulation and modifications of flavivirus structural proteins. J. Gen. Virol. https://doi.org/10.1099/vir.0.000097.

Rothan, H.A., Bidokhti, M.R.M., Byrareddy, S.N., 2018. Current concerns and perspectives on Zika virus co-infection with arboviruses and HIV. J. Autoimmun. https://doi.org/10.1016/j.jaut.2018.01.002.

Saiz, J.C., Vázquez-Calvo, Á., Blázquez, A.B., Merino-Ramos, T., Escribano-Romero, E., Martín-Acebes, M.A., 2016. Zika virus: The latest newcomer. Front. Microbiol. 7, 1–19.

Saiz, J.C., Martín-Acebes, M.A., 2017. The race to find antivirals for zika virus. Antimicrob. Agents Chemother. 61. https://doi.org/10.1128/AAC.00411-17.

Saiz, J.C., de Oya, N.J., Blázquez, A.B., Escribano-Romero, E., Martín-Acebes, M.A., 2018. Host-directed antivirals: a realistic alternative to fight zika virus. Viruses. https://doi.org/10.3390/v10090453.

Sharma, N., Dobhal, M., Joshi, Y., Chahar, M., 2011. Flavonoids: a versatile source of anticancer drugs. Pharmacogn. Rev. 5, 1. https://doi.org/10.4103/0973-7847.79093.

Song, B.H., Yun, S.I., Woolley, M., Lee, Y.M., 2017. Zika virus: history, epidemiology, transmission, and clinical presentation. J. Neuroimmunol. 308, 50–64. https://doi.org/10.1016/j.jneuroim.2017.03.001.

Stiasny, K., Fritz, R., Pangerl, K., Heinz, F.X., 2011. Molecular mechanisms of flavivirus membrane fusion. Amino Acids. https://doi.org/10.1007/s00726-009-0370-4.

Van Der Hoek, K.H., Eyre, N.S., Shue, B., Khantisitthiporn, O., Glab-Ampi, K., Carr, J.M., Gartner, M.J., Jolly, L.A., Thomas, P.Q., Adikusuma, F., Jankovic-Karasoulos, T., Roberts, C.T., Helbig, K.J., Beard, M.R., 2017. Viperin is an important host restriction factor in control of Zika virus infection. Sci. Rep. 7. https://doi.org/10.1038/s41598-017-04138-1.

Wang, Y., Gao, J., Miao, Y., Cui, Q., Zhao, W., Zhang, J., Wang, H., 2014. Pinocembrin protects SH-SY5Y cells against MPP+-induced neurotoxicity through the mitochondrial apoptotic pathway. J. Mol. Neurosci. 53, 537–545. https://doi.org/10.1007/s12031-013-0219-x.

WHO | World Health Organization, 2016. WHO statement on the first meeting of the International Health Regulations (2005) (IHR 2005) Emergency Committee on Zika virus and observed increase in neurological disorders and neonatal malformations. Who 37, 2–5.

Wu, Y., Cui, X., Wu, N., Song, R., Yang, W., Zhang, W., Fan, D., Chen, Z., An, J., 2017. A unique case of human Zika virus infection in association with severe liver injury and coagulation disorders. Sci. Rep. 7. https://doi.org/10.1038/s41598-017-11568-4.

Zandi, K., Teoh, B., Sam, S., Wong, P., Mustafa, M.R., 2011a. In vitro antiviral activity of Fisetin, Rutin and Naringenin against Dengue virus type-2. J. Med. Plants Res. 5, 5534–5539. https://doi.org/10.5897/JMPR11.1046.

Zandi, K., Teoh, B.T., Sam, S.S., Wong, P.F., Mustafa, M., Abubakar, S., 2011b. Antiviral activity of four types of bioflavonoid against dengue virus type-2. Virol. J. 8. https://doi.org/10.1186/1743-422X-8-560.

Zhang, J.H., Chung, T.D., Oldenburg, K.R., 1999. A simple statistical parameter for use in evaluation and validation of high throughput screening assays. J. Biomol. Screen 4, 67–73. https://doi.org/10.1177/108705719900400206.